Spontaneous spiral formation in two-dimensional oscillatory media

Petteri Kettunen,[1,2] Takashi Amemiya,[1] Takao Ohmori,[1] and Tomohiko Yamaguchi[1,2,*]
[1]*Department of Chemical Systems, National Institute of Materials and Chemical Research, Higashi 1-1, Tsukuba, Ibaraki 305-8565, Japan*
[2]*Department of Physical Sciences, Division of Biophysics, University of Oulu, Linnanmaa, FIN-90570 Oulu, Finland*
(Received 12 April 1999)

Computational studies of pattern formation in a modified Oregonator model of the Belousov-Zhabotinsky reaction is described. Initially inactive two-dimensional reaction media with an immobilized catalyst is connected to a reservoir of fresh reactants through a set of discrete points distributed randomly over the interphase surface. It is shown that the diffusion of reactants combined with oscillatory reaction kinetics can give rise to spontaneous spiral formation and phase waves. [S1063-651X(99)12708-9]

PACS number(s): 82.20.Mj, 47.54.+r, 82.20.Wt, 87.23.Cc

Spiral waves of excitation are observed in living and nonliving systems, such as the aggregation of the *Dictyostelium discoideum* slugs [1], Ca^{2+} waves in the cytoplasm of *Xenopus laevis* oocytes [2], catalytic CO oxidation on a Pt(110) surface [3], and the Belousov-Zhabotinsky (BZ) reaction [4,5]. However, in many cases the origin of their spontaneous appearance is not known. Particular studies of the BZ reaction have characterized the appearance of spiral waves under special conditions. It has been shown that the number of spirals can depend strongly on the excitability and cellular structure of the reaction media [6]. Geometrical constraints together with heterogeneous refractory properties can give rise to rotating vortices [7,8]. In ''numerical'' excitable media, turbulent spirals are reported in a discrete model showing analogy to cardiac physiology [9], and in a modified FitzHugh-Nagumo model with delayed-inhibitor production [10]. A pair of singular points with zero amplitude in oscillatory media is shown to create a nonuniform phase distribution that develops into a spiral wave [11].

Here we present computational studies of pattern formation in spatially distributed BZ reaction models with an emphasis on identifying some conditions that lead to spontaneous spiral formation. We consider a two-dimensional reaction medium, which initially contains only the immobilized catalyst. Then, the reaction medium is in contact with an ideal reservoir containing the other reactants for the BZ reaction (excess of BrO_3^-, H^+, Br^-, malonic acid, and other species). The lateral diffusion of reactants in the reaction medium is allowed to occur through a set of randomly distributed discrete points. Under the present conditions, the reaction is initiated when the reactants come into contact with the catalyst and the characteristic oscillations begin spontaneously. We show that the spatial coupling of both the diffusion of the reactants and the oscillatory kinetics gives rise to intricate pattern formation including rotating spiral segments and phase waves.

The reaction-diffusion model is based on the Tyson-Fife scaling of the two-variable Oregonator [12–14]. In order to account for the diffusion of reactants, one more equation is added to the model. The resulting three-variable system is given by

$$\frac{\partial u}{\partial \tau} = D_u \nabla^2 u + \frac{1}{\epsilon}\left(\hat{u} - \hat{u}^2 - f\, v\, \frac{\hat{u}-q}{\hat{u}+q} \right), \tag{1}$$

$$\frac{\partial v}{\partial \tau} = \hat{u} - v, \tag{2}$$

$$\frac{\partial r}{\partial \tau} = D_r \nabla^2 r, \tag{3}$$

where u and v describe the concentrations of $HBrO_2$ (activator) and oxidized catalyst (inhibitor), respectively, and $\nabla^2 = (\partial^2/\partial x^2) + (\partial^2/\partial y^2)$ is the two-dimensional Laplacian operator. Terms ϵ, q, and f are the standard parameters of the Tyson-Fife model [13,14], and D_u is the linear diffusion coefficient of $HBrO_2$. Variable r stands for the excitability relevant to the concentrations of the BZ reactants, and D_r is its corresponding linear diffusion coefficient. For simplicity, we introduce $\hat{u} = ur$ which models the linear coupling of the excitability and the reaction dynamics.

The main idea in the implementation of the model is that there are two types of diffusion sites on the integration grid. We define a site as one grid point (area Δ^2 in dimensionless units). Any given site is an *open site*, i.e., it is connected to the reservoir of reactants, with probability p, and a *closed site* with probability $1-p$. Therefore, the value of r at the open sites is kept at the maximum value $r_{\max}=1$ and constant throughout the simulation. In the initial state, the closed sites are given the value $r_{\min}=0$. For any definite system size with $0<p\leqslant 1$, the asymptotic solution of Eqs. (1–3) converges to that of the original two-variable Oregonator. Intuitively, it is clear that the saturated state is obtained faster with higher probabilities of p.

The kinetic parameters in our model were chosen as a combination of Tyson's ''Lo'' and Field-Förserling values: $q=0.002$ and $\epsilon=0.05$ [14–16]. Since we are interested in spontaneous pattern formation, the bifurcation parameter f was kept in oscillatory domain $f\leqslant 1.60$. If we consider soft-silica (water-glass) gel, the ratio of the diffusion coefficients D_r/D_u can be set at unity. In another gel, such as hard mesoporous silica gel (pore diameter appoximately 40 Å), the diffusion coefficients depend on the size of the hydrated mol-

*Author to whom correspondence should be addressed.

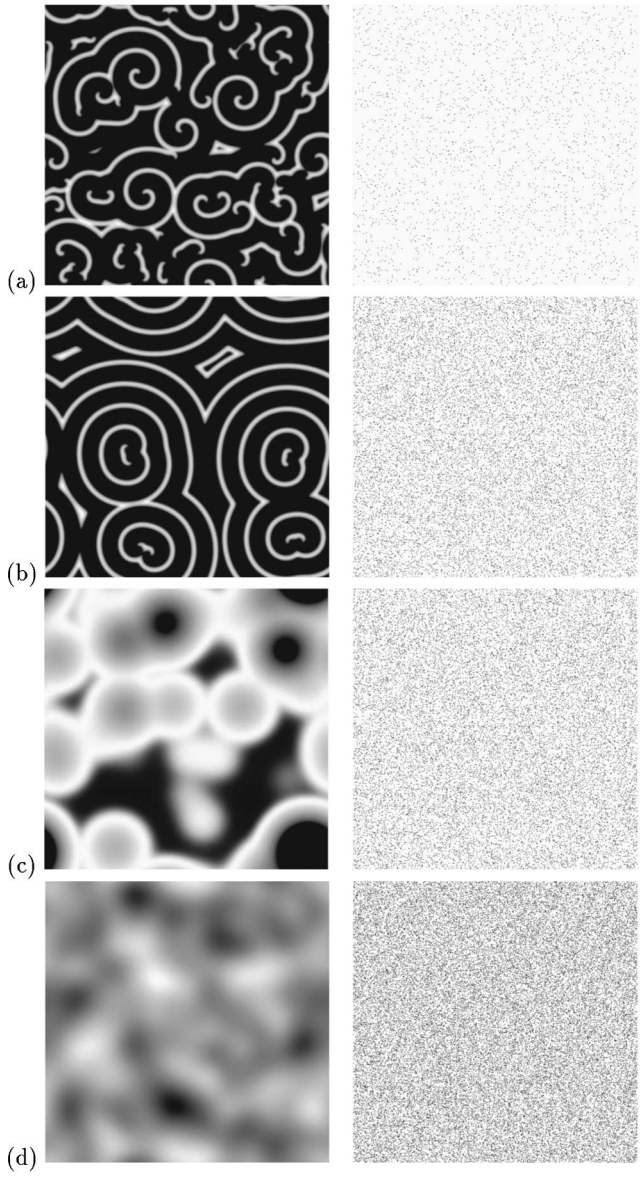

FIG. 1. Two-dimensional simulations of pattern formation with varying open diffusion site probabilities. Two images are shown for each example. The left-hand images show the dimensionless concentrations of the propagator u with white mapped to the highest value and black assigned to the steady-state value. On the right, black indicates the open diffusion sites. The open diffusion site probability p in each case is $p=0.0100$ (a); $p=0.0625$ (b); $p=0.0750$ (c); and $p=0.1500$ (d). The finite difference form of Eqs. 1–3 was integrated on a two-dimensional rectangular grid (periodic boundary conditions) with the forward Euler method using the standard five-point approximation for the Laplacian operator [34]. Parameters: $\epsilon=0.05$, $q=0.002$, $f=1.15$, $D_u=D_r=1$, grid size 512×512, grid spacing $\Delta=1/4$, time step $\delta\tau=7.8125\times10^{-4}$. The snapshots were collected after minimum 10×10^4 iterations. Decreasing the time step by a factor of 3 did not alter the simulated behavior.

ecule [17,18]. However, in Eq. (3) it is inclusively set that all the reactants have the same diffusivity. Therefore, only the case of equal diffusivities is considered.

Figure 1 shows typical examples of the simulations of Eqs. (1)–(3). With $p=0.0100$, the long-term behavior is characterized by chaotic spiral turbulence [Fig. 1(a)]. However, increasing p to 0.0625 decreases substantially the number of the spiral segments [Fig. 1(b)]. Increasing p further on changes remarkably the qualitative behavior of the system. Figure 1(c) shows spontaneous patterns arising from randomly distributed nucleation sites with $p=0.0750$. The activity resembles circular patterns, but since the nucleation sites are rather closely packed, the overall behavior is more like a mixture of stochastic oscillating domains and phase waves. Once p is brought high enough, e.g., $p=0.1500$, all of the distinguishable patterns disappear and the long-time behavior is characterized by large oscillating domains [Fig. 1(d)].

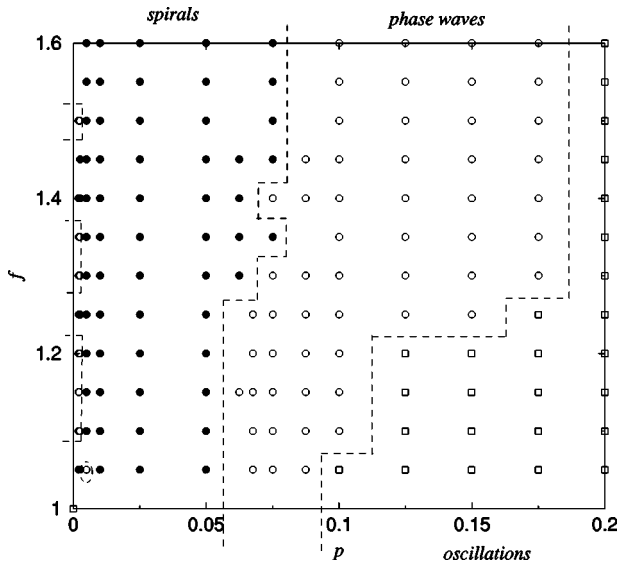

FIG. 2. Phase diagram showing pattern formation as a function of diffusion site probability and f value. Parameters are the same as in Fig. 1, except that grid size is 200×200. Simulations that required more than 15×10^4 iterations to reach 99% saturation level of the reactants were excluded. Symbols: ○, phase waves; ●, spirals; and □, oscillations.

Simulations carried out to determine the effects of the open site probability and excitability on pattern formation are summarized in Fig. 2. The phase diagram shows that no characteristic patterns were observed with p above some critical value. Once a condition is selected, $f=1.50$, pattern formation with increasing p goes from phase waves to spirals to phase waves and to oscillations. In a few cases at low p, phase waves preceded the appearance of spirals. The f value clearly affects the point of transition from one phase to another, although no substantial shifts were observed with these parameters.

The turbulent state accompanied with rotating spirals was subjected to closer examination. Shown in Fig. 3 is the number of spirals as a function of p (denoted by N). It can be clearly seen that there is a specific $p_{N,\max}$ where the maximum number of spirals is exhibited. With $f=1.05$ this value is $p_{N,\max}\approx0.0250$. When f is increased to 1.30, $p_{N,\max}\approx0.0275$, and with $f=1.60$, $p_{N,\max}\approx0.0300$. The maximum packing of spirals was obtained with the lowest value of $f=1.05$ investigated. As the f value increases, the maximum packing of spirals can appear at higher p.

The underlying mechanism responsible for the pattern formation in this model can be explained by considering the

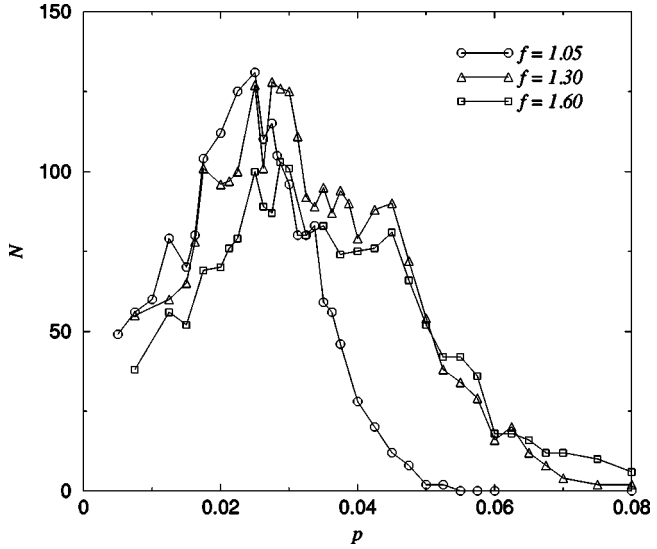

FIG. 3. Number of spirals N plotted as a function of p. The f value in each case is $f=1.05$ (○), $f=1.30$(△), and $f=1.60$ (□). Other parameters as in Fig. 1. N was determined by counting the vortices after a minimum of 10×10^4 iterations.

role of oscillations emitted from isolated clusters of open sites. Figure 4 shows how the phase difference in oscillations can be induced significantly depending on the effective size of a cluster of open diffusion sites. Oscillations begin immediately from an infinite cluster (cluster size $S=\infty$, i.e., initially homogeneous system) and in this example the period is $T=4.98\pm0.02$ [Fig. 4(a)]. The oscillations in the extreme opposite case of single isolated open site ($S=1$) start slowly after a long quiescent state [Fig. 4(b)]. Once the reactants have spread over the critical nucleation size (characterized in [19]), the active domain can support full oscillations and the

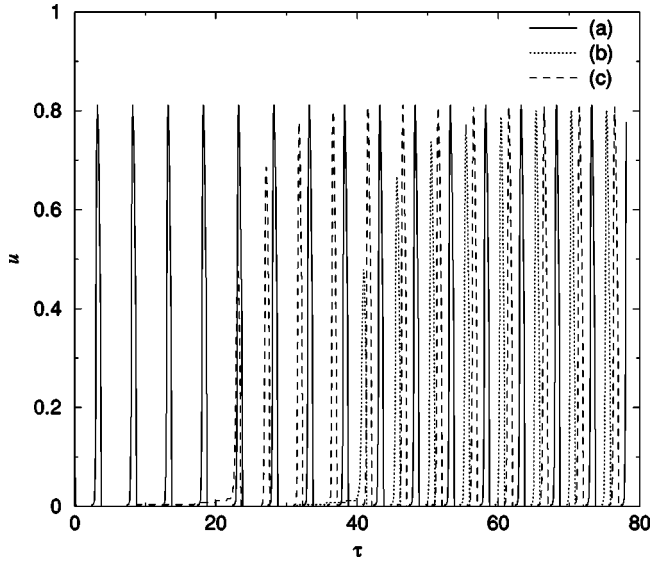

FIG. 4. Time traces of oscillating concentrations arising from isolated and symmetrical clusters of open diffusion sites. The cluster sizes are $S=\infty$ (a); $S=1$, i.e., single-diffusion site (b); $S=9$, i.e., a cluster of 3×3 sites (c). Kinetic and numerical parameters are as in Fig. 1, except $f=1.05$.

phase difference compared to the homogeneous system becomes approximately $T/3$. The dephasing is very sensitive to the cluster size, which can be seen from the resulting phase difference approximately $T/4$ between $S=1$ and $S=9$ [Figs. 4(b) and 4(c)]. There are also detectable alterations in the oscillation periods during the initial evolution.

At very low p, e.g., $p<0.001$, the clusters of open sites are nearly isolated from each other and the coupling length between the clusters is long. Therefore, the reaction domains can enlarge without perturbations from other clusters. Therefore, only oscillations are observed and no symmetry breaking occurs (data not shown). When the mean cluster size and the cluster perimeter increase, the diffusion from a cluster to its surroundings becomes faster in comparison with the oscillation period. Now the kinetic conditions and the phase of the oscillation can become remarkably different between the geometric center of the cluster area and the surrounding medium. This is the condition under which the dephasing waves appears [20]. Thus the dephasing of the oscillations in the spatial domain and the inherent refractory properties of the BZ reaction provide a foundation for the evolution of phase waves.

Based on these observations, we hypothesize that spirals appear when the deviations in cluster sizes are optimal for generating an ensemble of dephased oscillating domains. When these domains expand and become spatially coupled, the singularities in the spatial phase distribution [11] and the interaction of the phase wave fronts due to refractory and vulnerable properties [21–23] can form spiral cores. In addition, the differences in the oscillation periods (which can be seen in Fig. 4) enhance the mechanism due to vulnerability. Since the spirals in active media are high-frequency self-sustaining structures, they suppress the competing bulk oscillations and the system becomes dominated by rotating vortices. At high p, e.g., $p\geqslant0.200$, the clusters are large and the system is quickly saturated with reactants. Thus dephasing cannot occur to any significant degree and no distinctive patterns evolve.

The mechanism for pattern formation described here relies on the diffusion of reactants in an active non-linear reaction environment. It can be associated with several real systems ranging from fundamental physico-chemical models [24] to signal transport phenomena in cell activation [25,26] to explosive crystallization phenomena in amorphous films [27]. Phenomenologically, the model is analoguos to a commonplace BZ experiment, in which reaction solutions are poured on catalyst-loaded gel [17], vycor glass [18], or synthetic membranes [28]. Since the surface of the porous catalyst medium is never ideally homogeneous, it can generate random alterations of diffusion properties in spatial domains. As for the liquid phase, where the first BZ experiments were performed [4,5] , localized and random hydrodynamic forces can account for the generation of singularities in the spatial phase distribution, thus giving rise to spontaneous spiral waves.

Analogues of spiral waves in three dimensions are scroll waves [29,30]. Inevitably, an extended version of this model with three spatial dimensions can be helpful to study their spontaneous appearance. Chemical helix waves have been found to form spontaneously in a thin tube, filled with

catalyst-immobilized gel, whose open ends are in contact with BZ reactants [31]. Once a spiral is initiated on either of the two-dimensional surfaces, it can develop into a helicoidal wave with concentration gradients along the cylindrical axis. This scenario, which is in accordance with our model, has been predicted theoretically [32] and it is also seen in a biological medium [33].

One of the authors (P.K.) acknowledges the Science and Technology Agency of Japan.

[1] G. Gerisch, Naturwissenschaften **58**, 430 (1971).
[2] J. Lechleiter, S. Girard, E. Peralta, and D. Clapman, Science **252**, 123 (1991).
[3] R. Imbihl and G. Ertl, Chem. Rev. **95**, 697 (1995).
[4] A. Zaikin and A. Zhabotinsky, Nature (London) **225**, 535 (1970).
[5] A. Winfree, Science **175**, 634 (1972).
[6] J. Maselko and K. Showalter, Physica D **49**, 21 (1991).
[7] K. Agladze, J. Keener, S. Müller, and A. Panfilov, Science **264**, 1746 (1994).
[8] O. Steinbock, P. Kettunen, and K. Showalter, Science **269**, 1857 (1995).
[9] H. Ito and L. Glass, Phys. Rev. Lett. **66**, 671 (1991).
[10] M. Bär and M. Eiswirth, Phys. Rev. E **48**, R1635 (1993).
[11] D. Ueyama master's thesis, Ryukoku University, 1995.
[12] R. Field and R. Noyes, J. Chem. Phys. **60**, 1877 (1974).
[13] J. Tyson and P. Fife, J. Phys. Chem. **73**, 2224 (1980).
[14] J. Keener and J. Tyson, Physica D **21**, 307 (1986).
[15] R. Field and H.-D. Försterling, J. Phys. Chem. **90**, 5400 (1986).
[16] W. Jahnke, W. Skaggs, and A. Winfree, J. Phys. Chem. **93**, 740 (1989).
[17] T. Yamaguchi *et al.*, J. Phys. Chem. **95**, 5831 (1991).
[18] T. Amemiya, M. Nakaiwa, T. Ohmori, and T. Yamaguchi, Physica D **84**, 103 (1995).
[19] Á Tóth, V. Gáspár, and K. Showalter, J. Phys. Chem. **98**, 522 (1994).
[20] R. Aliev, T. Yamaguchi, and Y. Kuramoto, J. Phys. Chem. **101**, 7691 (1997).
[21] A. Babloyantz and J. Sepulchre, Physica D **49**, 52 (1991).
[22] M. Gómez-Gesteira *et al.*, Physica D **76**, 369 (1994).
[23] T. Amemiya, S. Kádár, P. Kettunen, and K. Showalter, Phys. Rev. Lett. **77**, 3244 (1996).
[24] G. Nicolis and I. Prigogine, *Self-Organization in Nonequilibrium Systems* (Wiley, New York, 1977).
[25] M. Kaufman, F. Andris, and O. Leo, in *Theoretical and Experimental Insight into Immunology*, edited by A. Perelson and G. Weisbuch (Springer-Verlag, Berlin, 1992), pp. 93–115.
[26] W. Kolanus, C. Romeo, and B. Seed, Cell **74**, 171 (1993).
[27] N. Provatas, M. Grant, and K. Elder, Phys. Rev. E **53**, 6263 (1996).
[28] A. Lázár, Z. Noszticzius, H. Farkas, and H.-D. Försterling, Chaos **5**, 443 (1995).
[29] A. Winfree, Science **181**, 937 (1973).
[30] A. Pertsov, R. Aliev, and V. Krinsky, Nature (London) **345**, 419 (1990).
[31] T. Yamaguchi and S. Müller, Physica D **49**, 40 (1991).
[32] A. Panfilov, A. Rudenko, and A. Pertsov, in *Self Organization—Autowaves and Structures Far From Equilibrium*, edited by V. Krinsky (Springer, Berlin, 1984), pp. 103–105.
[33] F. Siegert and C. Weijer, Proc. Natl. Acad. Sci. USA **89**, 6433 (1992).
[34] W. Press, B. Flannery, S. Teukolsky, and W. Vetterling, *Numerical Recipes in C* (Cambridge University Press, New York, 1992).